Precision Clinical Medicine, 2026, **9**: pbag001
https://doi.org/10.1093/pcmedi/pbag001
Published: 6 January 2026
Research Article

OXFORD

Antibiotic exposure impairs the efficacy of first-line chemoimmunotherapy in non-small cell lung cancer through the regulation of gut microbiome and bile acid metabolism

Hanyan Xu[1,‡], Jia Yu[2,‡], Lijing Xia[1], Xiong Lei[3], Liwen Zhou[1], Pengcheng Lin[1], Shanshan Su[1], Yuping Li[1,*], Chengshui Chen[1,2,4,*]

[1]Department of Pulmonary and Critical Care Medicine, The First Affiliated Hospital of Wenzhou Medical University, Wenzhou 325035, China
[2]Zhejiang Province Engineering Research Center for Endoscope Instruments and Technology Development, The Quzhou Affiliated Hospital of Wenzhou Medical University, Quzhou People's Hospital, Quzhou 324000, China
[3]Department of Emergency, The First Affiliated Hospital of Wenzhou Medical University, Wenzhou 325035, China
[4]Key Laboratory of Interventional Pulmonology of Zhejiang Province, The First Affiliated Hospital of Wenzhou Medical University, Wenzhou 325000, China
*Corresponding authors: Chengshui Chen, chenchengshui@wmu.edu.cn; Yuping Li, wzliyp@163.com
‡Hanyan Xu and Jia Yu contributed equally to this work.

Abstract

Objective: **Previous antibiotic therapy is acknowledged to potentially reduce the efficacy of single-agent immune checkpoint inhibitors. Nevertheless, the impact of antibiotics on the results for patients undergoing chemoimmunotherapy remains unclear. This research investigated the influence of antibiotic treatment on the effectiveness of chemoimmunotherapy in advanced non-small cell lung cancer (NSCLC).**

Methods: **We recorded the characteristics of patients with advanced NSCLC and assessed potential associations between the use of antibiotics and the efficacy of chemoimmunotherapy. A mouse model using Lewis lung carcinoma (LLC) cell lines was developed to assess the effects of antibiotics on the gut microbiome and metabolites. Fecal samples were analyzed using 16S rRNA gene sequencing and ultra-high-performance liquid chromatography–mass spectrometry (UHPLC-MS) methods. Mouse fecal and serum samples and 16 human stool samples were used to validate the identified differentially metabolites. Deoxycholic acid (DCA) was further applied to a LLC mouse model.**

Results: **This study included 387 NSCLC patients, among whom 86 patients had used antibiotics within the 30 days before the first cycle of chemoimmunotherapy (ATB group), and 301 patients had not used antibiotics (non-ATB group). Notable discrepancies were observed in overall survival and progression-free survival between the two groups, with overall survival recorded at 18.4 months versus 32.0 months, and progression-free survival at 7.6 months versus 13.0 months, in the ATB and non-ATB groups respectively. At the phylum level, the relative abundances of *Proteobacteria*, *Cyanobacteria*, and *Deinococcus* were increased in the ATB mice, while *Firmicutes*, *Bacteroidetes*, and *Verrucomicrobia* were decreased. We detected significant differences in DCA levels in the fecal and serum samples from mice as well as in the fecal sample from humans between the ATB and non-ATB groups. The respective proportions of CD4+ and CD8+ cells were greater in the non-ATB group than in the ATB group, whereas the proportion of Ki67-positive cells was greater in the ATB group. DCA was applied to LLC mice, and DCA along with chemoimmunotherapy effectively inhibited tumor growth in a LLC mouse model. The expression of programmed cell death ligand 1 increased in the DCA group.**

Conclusions: **Antibiotic exposure is associated with decreased efficacy of chemoimmunotherapy in patients with NSCLC via dysregulation of the gut microbiome and DCA metabolism.**

Keywords: non-small cell lung cancer, antibiotic, chemoimmunotherapy, metabolism, deoxycholic acid, gut microbiome

Received: 19 August 2025. **Revised:** 23 December 2025. **Accepted:** 3 January 2026

Introduction

Immunotherapy has transformed the treatment approach for advanced non-small cell lung cancer (NSCLC), with immune checkpoint inhibitors (ICIs) showing substantial enhancements in patient outcomes. Nonetheless, recent studies have brought to light the possible influence of antibiotic use on the effectiveness of ICIs, leading to varying responses to immunotherapy. Numerous investigations have indicated that receiving antibiotics, either prior to or during ICI therapy, correlates with reduced survival rates in NSCLC patients [1, 2]. A systematic review evaluating the impact of antibiotic exposure on survival in NSCLC patients receiving ICIs demonstrated a significant reduction in overall survival (OS) among those who had received antibiotics, with an average OS decrease of $>$6 months [3]. Similarly, a cohort study involving 291 patients with advanced cancer treated with ICIs found that even a single course of antibiotics was associated with a markedly shorter median OS, while multiple courses resulted in an even more pronounced decline [4].

Furthermore, the progression-free survival (PFS) and OS for NSCLC patients who took antibiotics within 30 days before starting ICI therapy were significantly reduced compared to those who did not receive antibiotics. Moreover, OS and PFS rates for NSCLC patients who received antibiotics within 30 days prior to beginning ICI therapy were notably lower than those of patients who did not undergo antibiotic treatment [5]. This effect seems to be more evident when antibiotics are consumed around the time ICI treatment begins.

The gut microbiome is increasingly acknowledged as an important factor in modulating ICI response, where its composition and functionalities affect the host's immune responses [6–8]. Antibiotics can modify the gut microbiome by decreasing microbial diversity, which might influence the effectiveness of ICIs. A recent investigation indicated that in NSCLC patients receiving only ICI treatment, high levels of *Intestinimonas* and the *Enterobacteriaceae* family correlated with significantly shorter PFS, with hazard ratios (HRs) of 2.61 ($P = 0.02$) and 3.34 ($P = 0.005$), respectively [6]. These results imply that gut microbiome might play a role in lung cancer patient prognosis by affecting immunotherapy effectiveness. Components of the gut microbiota and metabolites derived from them influence immune homeostasis both locally and systemically [9]. Pathway analyses, including Kyoto Encyclopedia of Genes and Genomes (KEGG) and Clusters of Orthologous Groups (COG), have shown that pathways related to sucrose and starch metabolism, as well as mannose and fructose metabolism, are diminished in the microbiome of lung cancer patients [10]. Alterations in the metabolism of intestinal flora in individuals with lung cancer may also impact immunotherapy outcomes. One recent study found a positive correlation between the abundance of the commensal bacterium *Lactobacillus johnsonii* and ICI response. Additionally, supplementation with *L. johnsonii* or the metabolite indole-3-propionic acid, derived from tryptophan, improved the effectiveness of anti-programmed death-1 antibody (αPD-1) immunotherapy mediated by CD8+ T-cells [11]. Variations in these metabolites influenced the metabolic pathways in lung cancer patients, which could subsequently affect immunotherapy efficacy. However, combinations of chemotherapy and immunotherapy have emerged as a robust first-line treatment option for many patients, independent of programmed cell death ligand 1 (PD-L1) expression, resulting in improved survival rates among those with metastatic NSCLC [12, 13]. Thus, there is currently no evidence supporting the notion that dysbiosis induced by antibiotics can alter outcomes in patients undergoing combined chemoimmunotherapy for advanced NSCLC.

In this study, therefore, we explored the effect of prior antibiotic exposure in chemoimmunotherapy recipients with advanced NSCLC and investigated the associations among antibiotic-mediated gut microbial imbalance, metabolite changes, and the efficacy of chemoimmunotherapy. To our knowledge, this is the first study to demonstrate that antibiotic-induced dysbiosis compromises the efficacy of chemoimmunotherapy through modulation of the gut microbiome–bile acid–immune axis, and that bile acid supplementation can restore antitumor immunity.

Materials and methods

Study population

This exploratory analysis was conducted in the Department of Pulmonary and Critical Care Medicine at the First Affiliated Hospital of Wenzhou Medical University, a tertiary educational facility located in Zhejiang, China. From January 2020 to August 2023, patients with histologically confirmed advanced NSCLC at stages IIIB–IVB who were treated with first-line ICIs alongside chemotherapy were included. The criteria for exclusion were: (i) individuals with other primary malignancies, (ii) those lacking consistent follow-up at our institution, and (iii) patients who underwent fewer than two treatment cycles. The conclusion of the follow-up period was set for 31 October 2024. The clinical outcomes measured included PFS, OS, and the objective response rate (ORR).

Considering prior evidence that indicates a time-dependent link between the administration of antibiotics and outcomes related to ICIs, the use of antibiotic therapy within the 30 days preceding the initiation of ICI treatment was selected as the main exposure metric. To evaluate concurrent medications, medical records were reviewed, with any systemic antibiotic treatments administered in the 30 days leading up to day 1 of the first cycle classified into the antibiotic (ATB) group. Detailed information on antibiotic exposure was available for 86 patients. Among these, 9 patients received oral antibiotics while 77 patients received intravenous antibiotics. The duration of antibiotic therapy was $>$7 days in 34 patients and was $\leq$7 days in 52 patients. The antibiotic classes administered included moxifloxacin ($n = 10$), ceftazidime ($n = 8$), ceftriaxone ($n = 20$), piperacillin-tazobactam ($n = 17$), cefoperazone-sulbactam ($n = 23$), latamoxef ($n = 6$), minocycline ($n = 1$), and mezlocillin-sulbactam ($n = 1$). Fecal samples from 16 patients were gathered prior to the commencement of the first cycle of chemoimmunotherapy. Approval for this research was granted by the institutional review board at the First Affiliated Hospital of Wenzhou Medical University (No. 2 020 084). All patients involved in this study signed informed consent forms.

Animal experiments

Animal-related procedures were carried out in accordance with the Institutional Laboratory Animal Research Guidelines and were approved by the Laboratory Animal Ethics Committee at the First Affiliated Hospital of Wenzhou Medical University. The experiments utilized 8-week-old female C57BL/6J mice of SPF grade,

acquired from the Vital River Experimental Animal Center in Beijing, China. These mice were maintained in a controlled environment with a 12-hr light/dark cycle at 25°C, having unrestricted access to food and water. Lewis lung carcinoma (LLC) cells were diluted to a concentration of 5×10^6 cells/ml, after which they were resuspended in 100 μl of phosphate-buffered saline (PBS) and administered via subcutaneous injection into the flanks of the mice. Tumor volumes were assessed 3 days post-injection, using Vernier calipers every 3 to 4 days. The volume calculations followed the formula $V = (L \times W \times W)/2$, where L signifies the tumor's length and W denotes its width. Upon reaching a tumor volume of $\sim$50 mm^3 in the initial cohort of animals, the mice were categorized into two distinct experimental groups. One group acted as the control, receiving 200 µl of 0.9% normal saline, while the second group was designated as the antibiotic group, receiving 200 µl of ceftriaxone sodium (Aladdin, China) that was dissolved in 0.9% normal saline at a concentration of 200 mg/ml per day. Ceftriaxone, a clinically relevant broad-spectrum β-lactam antibiotic, was selected based on its established ability to induce reproducible gut microbiota dysbiosis in mice with good systemic tolerability.

The second set of mice was randomly split into two subgroups: one receiving only chemoimmunotherapy and the other that had prior antibiotic treatment in addition to chemoimmunotherapy. Chemoimmunotherapy consisted of 10 mg/kg paclitaxel (PTX; Selleck, China) and 200 μg/kg anti-PD-1 antibody (Selleck, China) every 3 days for four cycles and was administered via intraperitoneal injection. Finally, the mice were sacrificed, and the tumors were photographed and measured.

In the second part of the study, the LLC mice were randomly divided into four groups: the control group [200 μl of sodium carboxymethyl cellulose administered by gavage for 7 days, then 200 μg/kg of IgG antibody (Selleck, China) administered intraperitoneally every 3 days], the deoxycholic acid (DCA) group [50 mg/kg of DCA (Sigma, USA) administered by gavage for 7 days, then 200 μg/kg of IgG antibody (Selleck, China) administered intraperitoneally every 3 days], the PTX and anti-PD-1 antibody group [200 μl of sodium carboxymethyl cellulose administered by gavage for 7 days, then 200 μg/kg of anti-PD-1 antibody (Selleck, China) and 10 mg/kg PTX administered intraperitoneally every 3 days], and the DCA combined with PTX and anti-PD-1 antibody group (50 mg/kg DCA administered by gavage for 7 days, then 200 μg/kg of anti-PD-1 antibody and 10 mg/kg PTX administered by intraperitoneal injection every 3 days), which were treated for a total of 3 weeks. The growth of the subcutaneously grafted tumors in the mice was observed every 2 days, and the tumor volume was measured and calculated. Finally, the mice were sacrificed, and the tumors were photographed and measured.

Sample collection

Fecal specimens were gathered from patients prior to the initiation of cycle 1 of chemoimmunotherapy. Blood specimens were drawn into collection tubes that contained ethylenediaminetetraacetic acid and subsequently centrifuged at 4000 $\times$ g for 15 min at 4°C to isolate serum. Subsequent to this, the serum samples were preserved at −80°C without undergoing multiple cycles of freezing and thawing prior to metabolite extraction. Fresh tissues were promptly snap-frozen and maintained at −80°C or alternatively fixed and embedded in paraffin.

Fecal microbiome analysis by 16S rRNA sequencing

The amplification of 16S rRNA genes from various regions (16SV4) was conducted using specific barcoded primers (16SV4: 515F-, 806R). The PCR reactions were prepared by combining 15 µl of Phusion® High-Fidelity PCR Master Mix with specific concentrations of the primers. Both the forward and reverse primers were utilized at a concentration of 0.2 µM, along with $\sim$10 ng of template DNA. The thermal cycling protocol commenced with a primary denaturation step at 98°C for 1 min, which was succeeded by a total of 30 cycles. An equivalent volume of 1X loading buffer and SYBR Green was combined with the PCR outcomes, after which electrophoresis was performed on a 2% agarose gel for visualization. The PCR products were equally pooled, and this mixture was subsequently purified. Sequencing libraries were created, incorporating indices. A Qubit assay and real-time PCR were employed to assess the library's quality for quantification, while a bioanalyzer was used to determine size distribution. The libraries that were quantified were combined and sequenced using Illumina platforms, considering the effective concentration of the libraries and the necessary data volume.

Liquid chromatography-mass spectrometry-based fecal and blood metabolomics analyses

Untargeted ultra-high-performance liquid chromatography–tandem mass spectrometry

Samples were analyzed using Shimadzu CBM-30A Lite LC system (Shimadzu Corporation, Japan) in combination with a Waters Acquity HSS T3 column (2.1 $\times$ 100 mm, 1.8 μm), which is compatible with the API 6600 Triple TOF (AB Sciex, USA) mass detector. The methods and data processing approaches were modified from the protocol defined by Xiong [14] and customized to fit our specific needs; additional information can be found in the online supplementary material. Data was collected using the MassHunter workstation software, which then converted it into mzXML format. Subsequently, preprocessing of the data was performed using XC-MS software (XC-MS plus, USA), involving activities such as nonlinear retention time alignment, filtering, peak detection, matching, alignment, and identification.

Analysis of data and identification of metabolites

Before conducting single or multivariate data analyses, all liquid chromatography–mass spectrometry (LC-MS) data underwent normalization based on the sum and Pareto scales. The software SIMCA 14.1 (Umetrics, Sweden) was utilized to conduct multivariate analyses, which included orthogonal partial least squares discriminant analysis (OPLS-DA) as well as principal component analysis (PCA). While PCA provides a visual representation of the distribution features within the dataset, the OPLS-DA model is designed to differentiate between categories, elucidate the differences among group samples, and generate corresponding variable importance projection (VIP) values. To prevent overfitting, model validation was accomplished through a permutation test ($n = 200$). The performance of the model can be assessed with R^2Y and Q^2 values, where R^2Y reflects model accuracy and Q^2 in-

dicates predictive capability; as these parameter values approach 1.0, the reliability of the model increases. Statistical evaluations involving a single variable were performed using the online resource (https://www.omicshare.com/tools/).

Variables that met the criteria of a false discovery rate (FDR) < 0.05, VIP values > 1.0, and a fold-change (FC) < 0.5 or > 2 were categorized as metabolites with significant differential abundance. After identifying these significant metabolites, the subsequent identification phase was based on accurate m/z values and the signature fragments from MS/MS analysis, with validation carried out using HMDB 4.0.

Targeted ultra-high-performance liquid chromatography–tandem mass spectrometry

To quantify DCA in human feces, mouse feces, and serum samples, a targeted assay was employed. The analyses were performed using Shimadzu CBM-30A Lite LC system in conjunction with an API 6500 Q-TRAP (AB Sciex, USA) mass detector. For the separation process, a Waters Acquity HSS T3 column (2.1 $\times$ 100 mm, 1.8 μm) was utilized. The comprehensive protocol is available in the online supplementary material.

Standard solutions of DCA (Sigma-Aldrich) were prepared with concentrations varying from 0.5 to 1000 ng/ml, allowing for the establishment of concentration calibration curves. The quantification of metabolite concentrations was carried out with the help of AB Sciex MultiQuant software (version 2.1; AB Sciex, CA, USA).

Immunohistochemistry of tumor tissues and antibody assessment

Tumor tissue samples from the mice underwent histopathological examination. These samples were preserved in 4% paraformaldehyde for 48 h, followed by a gradient dehydration process, paraffin embedding, and cutting into sections with a thickness of 4 μm. Subsequently, the sections were processed for hematoxylin and eosin (H&E) staining, along with the detection of antibodies for CD4 (Abcam, UK, ab183685), CD8 (Abcam, UK, ab217344), and Ki67 (Cell Signaling Technology, USA, 12202T).

Statistical analysis

Statistical analysis was carried out with SPSS software version 22.0 (IBM Inc., Chicago, IL, USA). To evaluate the differences in continuous variables, unpaired two-sample t-tests were applied. The examination of nominal variables involved the use of chi-square and Fisher's exact tests. One-way analysis of variance (ANOVA) was used to determine differences between multiple groups. The Kaplan–Meier method, along with the log-rank test, was used to assess PFS and OS. The connections between gut microbiota and metabolites were examined through Pearson correlation analysis. All statistical evaluations were performed as two-sided tests, with a significance level set at a P-value < 0.05.

Results

Characteristics of patients

A total of 387 individuals participated in this study, comprising 44 females and 343 males. Among these patients, 270 (69.8%) were identified as smokers. The clinical attributes of all participants are presented in supplementary Table 1, see online supplementary material. In the study, 301 patients were categorized into the non-ATB group, while 86 were assigned to the ATB group. Both groups exhibited comparable characteristics regarding age, gender, Eastern Cooperative Oncology Group performance status (ECOG-PS) score, disease stage, potential metabolic conditions, tumor subtype, and smoking habits. Additionally, the prevalence of comorbidities such as diabetes was not significantly different between the two groups.

Efficacy of chemoimmunotherapy in the ATB group and non-ATB group

The ORR of the ATB group was 53.5% including 46 partial response (PR), 6 progression disease (PD) and 34 stable disease (SD), and the ORR of the non-ATB group was 65.1% (196 PR, 101 SD, 4 PD) ($P = 0.049$). The PFS of the ATB group was 7.6 months [95% confidence interval (CI): 5.7–9.5 months], which was significantly shorter than that of the non-ATB group [13.0 months (95% CI: 11.0–15.1 months)], $P < 0.001$, (HR = 1.61 (95% CI: 1.24–2.09)] (Fig. 1A). The OS of the ATB group was 18.4 months (95% CI: 12.2–24.5 months) and that of the non-ATB group was 32.0 months (95% CI: 26.8–37.2 months, $P < 0.001$) (HR = 2.15 (95% CI: 1.58–2.92)] (Fig. 1B).

Twelve patients (14.0%) in the ATB group and fifteen patients (5.0%) in the non-ATB group received antibiotics during subsequent treatment cycles. Analysis excluding these patients yielded similar results, supporting the robustness of the observed association.

To further determine whether this association was independent of other clinical factors, a multivariate Cox proportional hazards regression analysis was conducted, adjusting for age, gender, ECOG-PS, PD-L1 tumor proportion score (TPS) level, smoking history, ICI regimen type, and metastatic sites (liver, brain, and bone).

The results demonstrated that antibiotic exposure remained an independent predictor of both shorter PFS (HR = 1.55, 95% CI: 1.12–2.15, $P = 0.009$) and OS (HR = 2.17, 95% CI: 1.44–3.28, $P < 0.001$). In addition, bone metastasis was significantly associated with poor outcomes (PFS HR = 1.76, 95% CI: 1.32–2.35, $P < 0.001$; OS HR = 2.08, 95% CI: 1.43–3.04, $P < 0.001$), while older age was also linked to inferior OS (HR = 1.03, 95% CI: 1.00–1.05, $P = 0.042$). Other factors including gender, ECOG score, PD-L1 TPS, smoking history, and ICI type were not significantly associated with survival outcomes (supplementary Table 2, see online supplementary material).

Antibiotics promote tumor growth in an NSCLC mouse model receiving chemoimmunotherapy

In this study, we subcutaneously injected LLC cells into C57BL/6 mice to establish a xenograft model. The mice were randomly divided into four groups: the control (CON); ATB; αPD-1 + PTX; and ATB + αPD-1 + PTX groups (Fig. 2A). As shown in Fig. 2B and C, compared with that in the PTX + αPD-1 group, tumor vol-

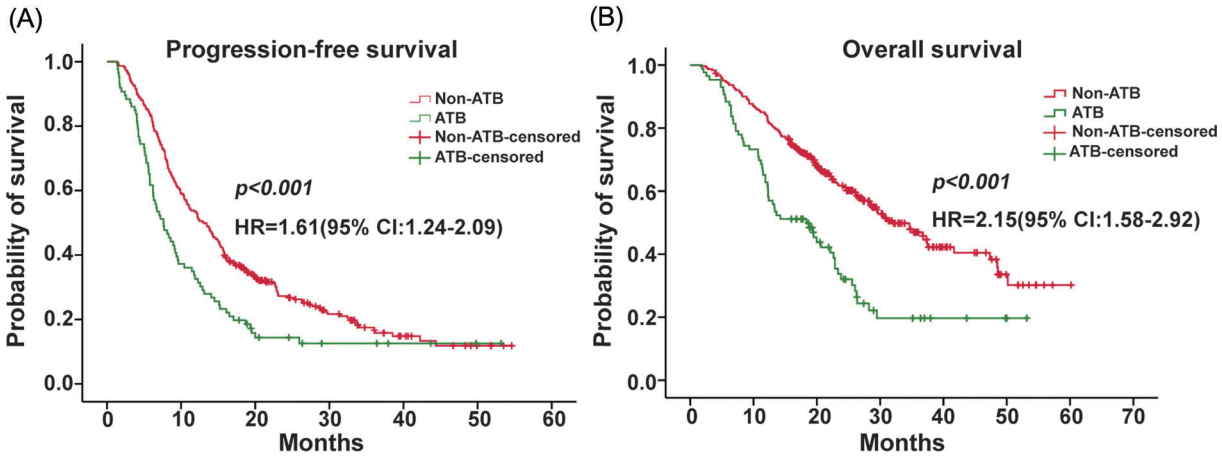

Figure 1 Kaplan–Meier survival estimate according to ATB. (A) PFS of non-ATB and ATB groups of advanced NSCLC receiving first-line chemoimmunotherapy. ATB: 7.6 months (95% CI: 5.7–9.5 months), non-ATB: 13.0 months (95% CI: 11.0–15.1 months). (B) OS of non-ATB and ATB group of advanced NSCLC receiving first-line chemoimmunotherapy. ATB: 18.4 months (95% CI: 12.2–24.5 months), non-ATB: 32.0 months (95% CI: 26.8–37.2 months).

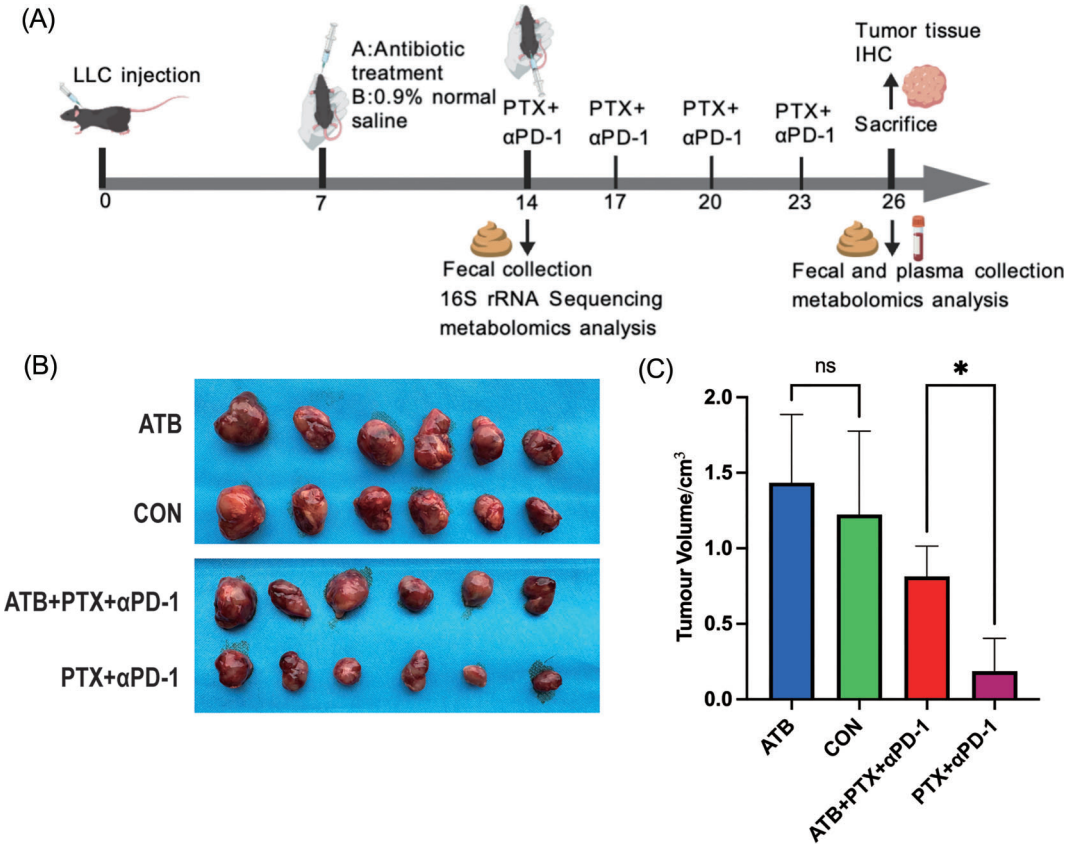

Figure 2 Antibiotics promote the growth of lung cancer cells in female C57BL/6 wild-type mice receiving chemoimmunotherapy. (A) Schematic diagram showing the process of antibiotic treatment and αPD-1 immunotherapy combined with PTX chemotherapy in the subcutaneous LLC xenograft tumor model. (B) Images of the tumors in the different groups. (C) Tumor volume after death. $*P < 0.05$; ns: not significant; CON: control.

ume was significantly greater in the ATB + PTX + αPD-1 group ($P = 0.036$), indicating that the combination of antibiotics and chemoimmunotherapy has inferior antitumor effects. There was no significant difference observed between the ATB and CON groups ($P = 0.440$).

Exposure to antibiotics affects the gut microbiota in mice

The analysis of mouse fecal samples was conducted using 16S rRNA sequencing to detect the gut microbiota. Through Illumina

sequencing, an average of 102 999 total microbial 16S rRNA reads were obtained from the fecal material for microbiome analysis, of which the combined number of reads was 102 527 and the combined percentage was 99.5%. The results revealed that the diversity (Fig. 3A) of the gut microbiota in feces was significantly lower in ATB mice than in CON mice.

Exposure to antibiotics led to notable reductions in the diversity of the gut microbiota in mice (Fig. 3A, $P < 0.001$).

An overview of the microbial profile at the phylum level is presented in Fig. 3B, indicating that the microbial composition in the ATB mice was distinct from that of the CON mice. Following antibiotic administration, a marked difference in microbial composition was noted in ATB mice compared to CON mice, with declines in the relative abundances of *Firmicutes*, *Bacteroidetes*, and *Verrucomicrobia*, alongside increases in *Proteobacteria*, *Cyanobacteria*, and *Deinococcota* (Fig. 3B and C). When examining community similarity, both principal coordinate analysis (PCoA) and nonmetric multidemensional scaling (NMDS) demonstrated that the application of antibiotics had a significant impact on the overall microbial composition in the mice (Fig. 3D and E). The microbes that significantly differed between CON and ATB mice at the genus level are shown in Fig. 3F, which shows that the abundances of *Acinetobacter*, *Escherichia-Shigella*, *Ahermus*, *Achromobacter*, and *Cupriavidus* were increased in ATB mice; however, the abundances of *Prevotellaceae_UCG-001*, *Ligilactobacillus*, *Ileibacterium*, *Alistipes*, and *Muribaculum* were decreased after antibiotic treatment (Fig. 3F).

Analysis of feces and plasma metabolism patterns in mouse models

Untargeted metabolomics and analysis of multivariate data

In this research, we utilized LC-MS to conduct comprehensive metabolic profiling of fecal samples collected from mice. We identified a total of 3 645 feature peaks in the electrospray ionization (ESI) positive mode and 4 066 feature peaks in the ESI− mode. The quality control samples exhibited a tight clustering on the PCA plot, demonstrating the instrument's strong analytical repeatability and stability (Fig. 4A and B). To assess metabolic profile variations between the ATB and CON mice, PCA was executed on all samples (Fig. 4A and B). The OPLS-DA score plots showed a distinct separation between the ATB and CON mice in both ESI+ and ESI− modes (Fig. 4C and D), with satisfactory fitting and predictive capability (ESI+: $R^2Y = 0.98$, $Q^2 = 0.95$; ESI−: $R^2Y = 0.99$, $Q^2 = 0.97$). A comparison of the ATB group after receiving treatment with PTX and αPD-1 against the CON group under similar treatment conditions indicated significant differences (supplementary Fig. 1C, ESI+: $R^2Y = 0.93$, $Q^2 = 0.81$; supplementary Fig. 1D, ESI-: $R^2Y = 1$, $Q^2 = 0.86$, see online supplementary material). To verify the OPLS-DA model for overfitting, we executed 200 permutation tests through SMICA-P and produced permutation plots. The findings showed no overfitting risk, as the substituted R^2 and Q^2 values were lower than the original ones, and the intercept of the regression line on the *y*-axis was negative (Fig. 4E and F).

Differentially abundant metabolites were identified based on a VIP > 1 and an FDR < 0.05. In the ESI+ mode, no metabolites within the CON and ATB groups satisfied both criteria. For analyzing the ESI- metabolites, volcano plots were utilized, as illustrated in Fig. 4G and H.

Quantification of metabolites

In this study, DCA was identified as the most significantly altered metabolite from the volcano plots. Subsequently, the DCA level in the fecal and plasma samples in mice and human fecal samples was accurately determined via an ultra-high-performance liquid chromatography–tandem mass spectrometry (UHPLC-MS/MS) targeted analysis method. The box-and-whisker plots in Fig. 5A and B and supplementary Fig. 2A and B (see online supplementary material) show that the concentration of DCA in the ATB group was lower than that in the CON group ($P = 0.0006$, $P < 0.0001$), and the DCA level in the ATB group after chemoimmunotherapy was also significantly lower than that in the CON group during the same period in both mouse fecal and serum samples ($P = 0.0356$, $P = 0.029$, respectively). We also validated these findings in the feces of human patients, and the results suggested that the DCA concentration decreased significantly after antibiotic treatment ($P = 0.0017$) (Fig. 5C).

Correlation between the gut microbiota and DCA

Analysis of the gut microbiota at the phylum level and DCA levels indicated that the *Bacteroidota* group was positively correlated with DCA, whereas the *Proteobacteria*, *Cyanobacteria*, *Deinococcota*, *Chloroflexi*, *Gemmatimonadota*, and *Acidobacteriota* were negatively correlated with DCA (supplementary Fig. 3A, see online supplementary material). Moreover, the results at the genus level revealed that *Enterococcus*, *Escherichia-Shigella*, and *unidentified_Chloroplast* were negatively correlated with DCA (supplementary Fig. 3B). Conversely, *Allobaculum*, *Dubosiella*, *Lactobacillus*, and *Prevotellaceae_UCG.001* were positively correlated with DCA (supplementary Fig. 3B). The detailed correlation indices and *P* values can be found in the online supplementary material.

DCA inhibits the growth of lung cancer mouse models receiving chemoimmunotherapy

We injected LLC cells subcutaneously into C57BL/6 mice to establish a xenotransplantation model. Subsequently, the tumor-bearing mice were randomly divided into four groups: CON group, DCA group, PTX + αPD-1 group, and DCA + PTX + αPD-1 group (supplementary Fig. 4A, see online supplementary material). As shown in supplementary Fig. 4B and C, tumor volume in the DCA + PTX + αPD-1 group was significantly reduced compared with the PTX + αPD-1 group ($P = 0.036$), indicating that DCA combined chemoimmunotherapy has better anti-tumor effects. In addition, there was no significant difference in tumor volume between the DCA group and the CON group ($P = 0.595$).

Immunohistochemistry of mouse tumor tissue

In this study, CD4 T cells, CD8 T cells, and Ki67 (a marker of tumor cell proliferation) were examined in the tumor tissue of 12 mice:

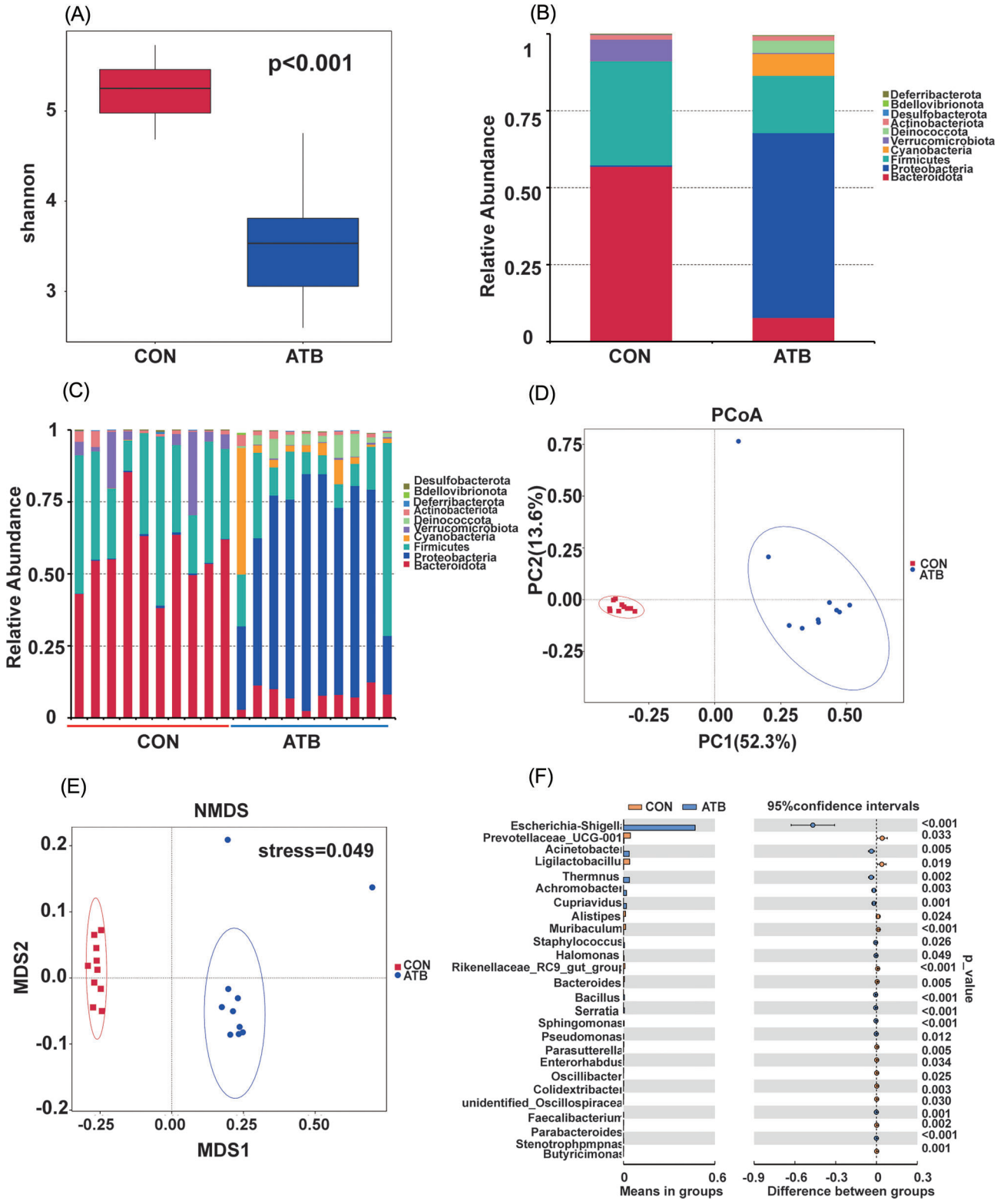

Figure 3 Gut microbiota in mice is modified by antibiotic exposure. (A) Shannon index for the control (CON) group and the antibiotic (ATB) group. (B) Community structures of microorganisms at the phylum level across different groups ($n = 10$ mice per group). (C) Relative abundance of gut microbiota at the phylum level in feces of each sample. (D) Principal coordinate analysis (PCoA) for each group. (E) Nonmetric multidimensional scaling (NMDS) analysis for the different groups. (F) Microbial taxa that exhibited significant changes between the CON and ATB groups.

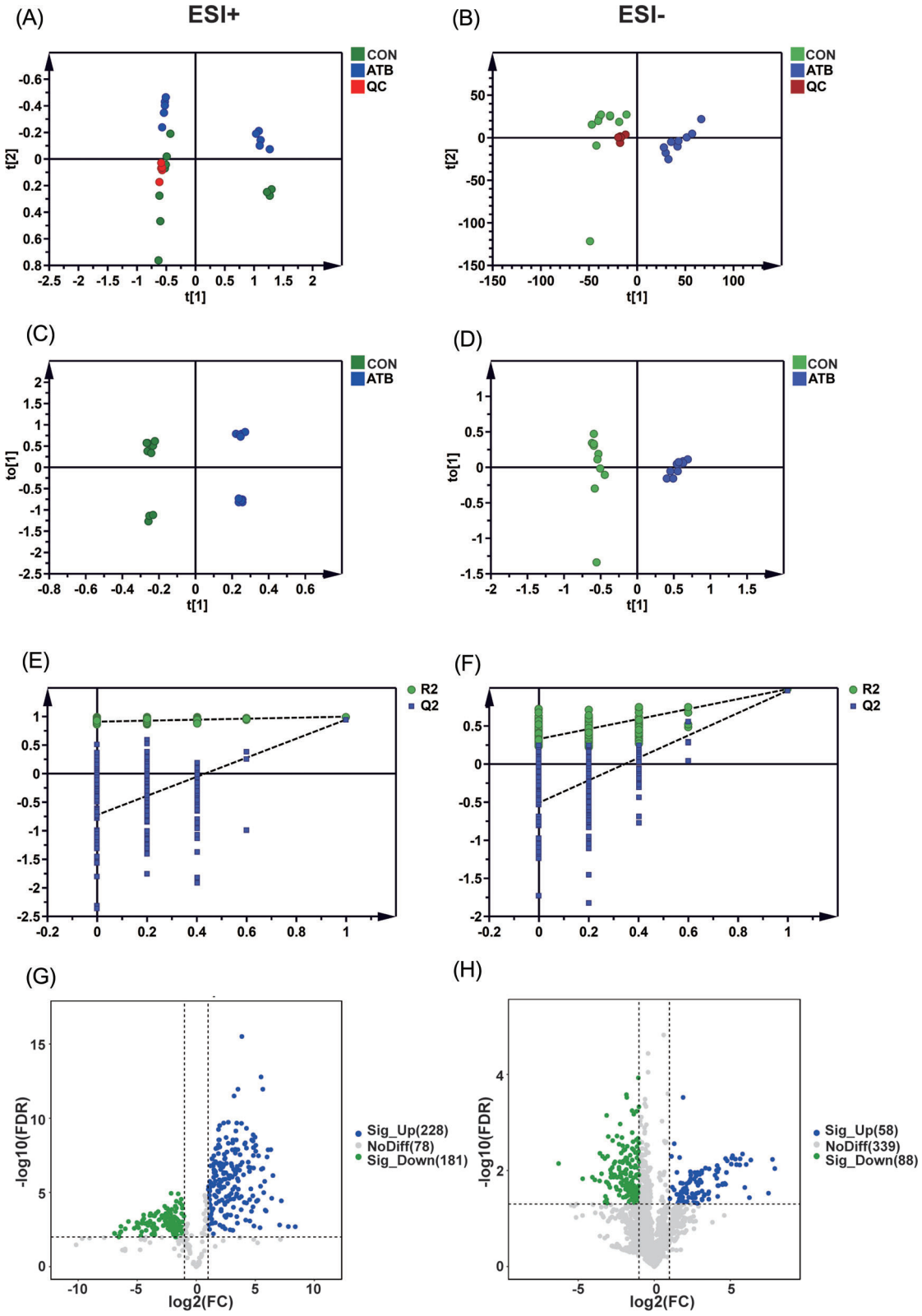

Figure 4 Multivariate data analysis and untargeted lipidomics. Utilizing LC–MS for untargeted metabolomics facilitates a comprehensive metabolic profiling of mouse feces, including PCA and OPLS-DA score maps that compare fecal samples from the control and antibiotic groups. (A) PCA maps in ESI+ patterns, (B) PCA maps in ESI− patterns, (C) OPLS-DA score maps in ESI+ patterns with $R^2Y = 0.98$ and $Q^2 = 0.95$, and (D) OPLS-DA maps in ESI− patterns with $R^2Y = 0.99$ and $Q^2 = 0.97$. (E and F) Validation plots derived from 200 alignment tests. (G and H) Metabolites with VIP > 1 and FDR < 0.05 were chosen, and volcano plot analysis was employed to highlight significant metabolites identified in ESI− (G) across the CON and ATB groups, as well as in ESI− (H) for the PTX + αPD-1 group and ATB + PTX + αPD-1 group.

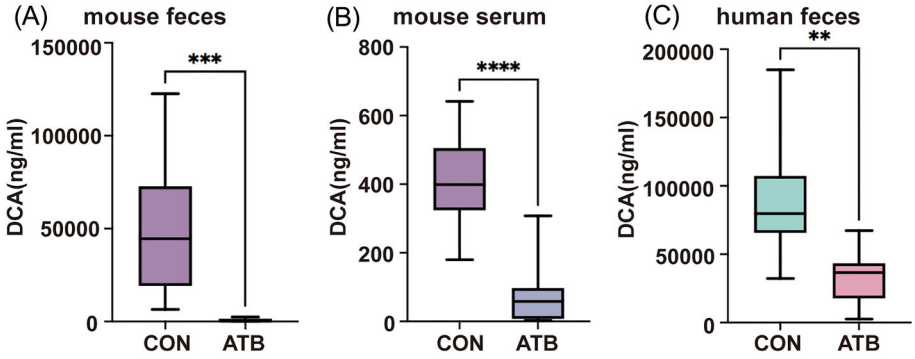

Figure 5 DCA content in (A) mouse feces, (B) mouse serum, and (C) human feces samples determined by UHPLC-MS/MS targeted analysis method using the DCA standard. $^{**}P < 0.01$, $^{***}P < 0.001$, $^{****}P < 0.0001$.

3 mice in the CON group, 3 mice in the ATB group, 3 mice in the PTX + αPD-1 group, and 3 mice in the ATB + PTX + αPD-1 group (Fig. 6). The proportion of neoplastic cells with nuclear positivity was determined. The results revealed that compared with the CON group, there was greater infiltration of Ki67 in the ATB group ($P = 0.007$), whereas the proportions of CD4+ T cells ($P = 0.010$) and CD8+ T cells ($P < 0.001$) were lower. Similarly, after chemotherapy combined with immunotherapy, Ki67 expression increased ($P = 0.008$), and CD4 and CD8 expression decreased in the ATB group ($P = 0.002$, $P < 0.001$).

The results show that the infiltration rate of Ki67 in the CON group was significantly higher than that in the DCA group ($P = 0.020$). CD4+ T cells and CD8+ T cells were significantly increased in the DCA group ($P = 0.003$, $P = 0.0036$, respectively). Similarly, the expression of Ki67 in the DCA combined with chemoimmunotherapy group was lower than that in the simple chemoimmunotherapy group ($P = 0.045$). CD4 and CD8 were significantly increased in the DCA combined with chemoimmunotherapy group ($P = 0.035$, $P = 0.0154$, respectively) (Fig. 7). The expression of PD-L1 in the DCA group was higher than that in CON group ($P = 0.009$) (Fig. 8), indicating that DCA increased the expression of PD-L1.

Discussion

Previous studies have reported the temporal aspect of how ATB exposure relates to outcomes from ICIs. These findings suggest that only previous exposure to ATB, rather than simultaneous exposure, is linked to poorer response rates and survival outcomes [5, 15]. Therefore, we chose the 30 days prior to the initiation of chemoimmunotherapy, as the time of antibiotic exposure. Subsequent antibiotic use during therapy was excluded from group classification due to the heterogeneous timing and indications. This study analyzed the clinical data of 387 patients with NSCLC who received first-line chemoimmunotherapy. In comparison to participants in clinical trials, the population in our study exhibited comparable oncological results. Compared with clinical trial participants, our study population experienced similar oncological outcomes [16]. We found that patients who had used systemic antibiotics within 30 days before the start of combined chemotherapy and immunotherapy had shorter PFS and OS than those who had not used antibiotics. This finding suggests that antibiotics may have a negative effect on the efficacy of chemoimmunotherapy. Although previous studies have shown that the use of antibiotics may affect the efficacy of immunotherapy for treating lung cancer, few studies have investigated the impact of antibiotics on the efficacy of chemotherapy combined with immunotherapy, and the conclusions were inconsistent. Our results provided new evidence in this field, emphasizing the importance of considering antibiotic use when planning and executing immunotherapy regimens for NSCLC patients and highlighting the need for further research to fully understand these interactions and their clinical implications [17, 18].

Our study using a mouse LLC subcutaneous tumor model further revealed significant changes in the composition of the gut microbiota after the use of antibiotics. The diversity of the gut microbiota significantly decreased after the use of antibiotics, a result that is consistent with previous studies [19]. Ceftriaxone was selected as a representative broad-spectrum antibiotic to induce gut microbial dysbiosis in mice, consistent with clinical antibiotic exposure patterns. However, we acknowledge that this model does not fully represent the diversity of antibiotic regimens employed in cancer patients. Additionally, we found that the abundance of potentially beneficial bacteria such as *Firmicutes*, *Bacteroidetes*, and *Verrucomicrobia* decreased, whereas the abundance of potentially harmful bacteria such as *Proteobacteria*, *Cyanobacteria*, and *Deinococcota* increased after the use of antibiotics. These changes are consistent with previous research results [20]. These results suggest that antibiotics may affect the efficacy of chemoimmunotherapy by altering the composition of the gut microbiota. Notably, while the CON group exhibited higher CD4+/CD8+ infiltration compared to the ATB group, their tumor volumes were similar at the time of sampling. This observation likely reflects the earlier onset of immune recruitment in relation to measurable tumor regression. In the PTX + αPD-1 group, Ki67 expression remained comparable to that of the control group, whereas CD4+/CD8+ infiltration was lower. This pattern likely indicates an early treatment phase during which tumor proliferation had already been constrained, while immune re-infiltration and effector T-cell expansion were still in progress. In comparison, Fig. 7 illustrates that DCA supplementation not only restored but also enhanced CD4+/CD8+ T-cell infiltration while simultaneously reducing Ki67 levels. This finding supports the role of the gut microbiome–bile acid axis in shaping the tumor immune microenvironment. Furthermore, DCA supplementation partially mitigated the antibiotic-induced suppression of antitumor immunity, as evidenced by increased infiltration of CD4+ and CD8+ T

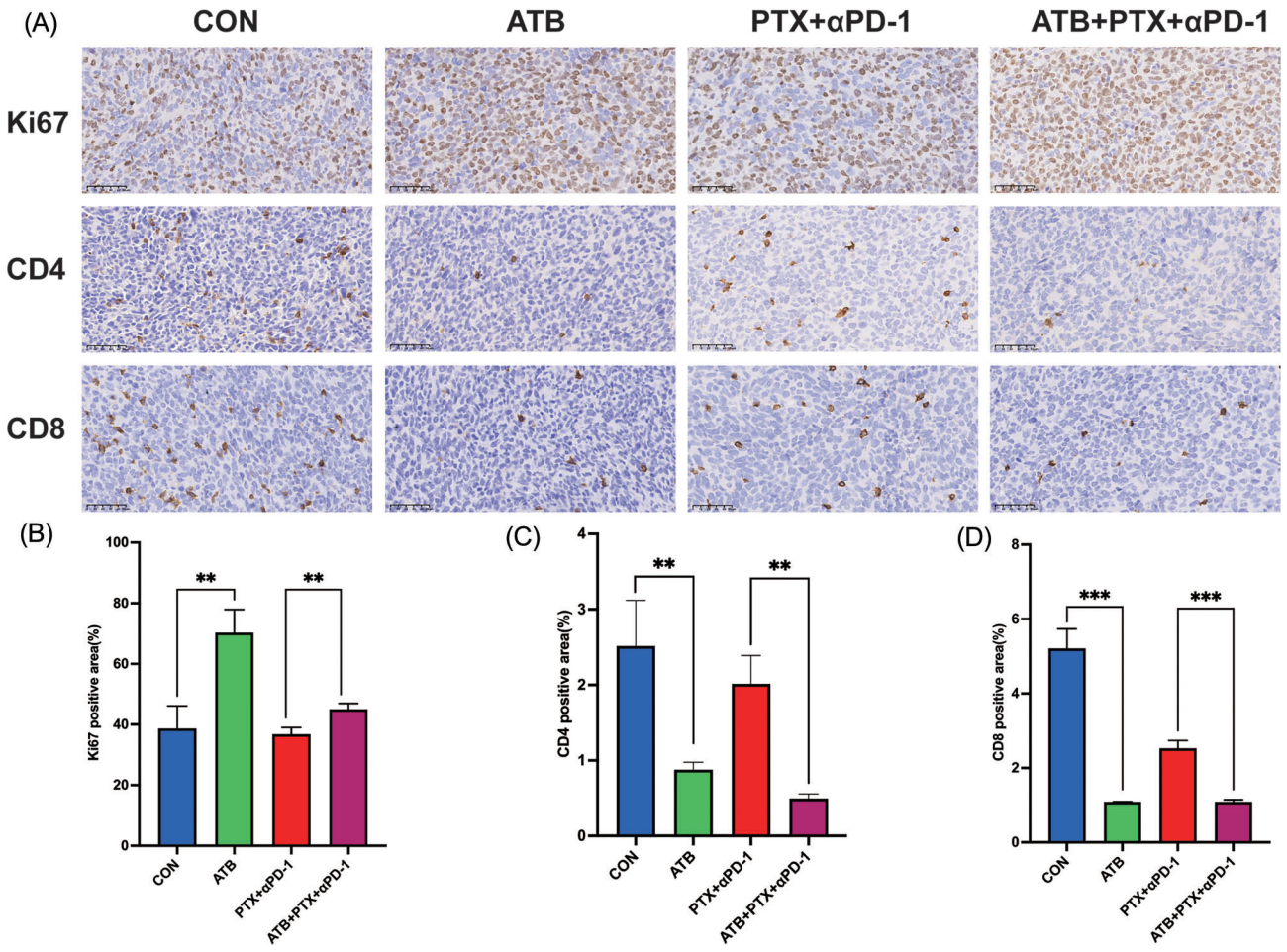

Figure 6 (A) Immunohistochemical images of Ki67, CD4, and CD8 in subcutaneous tumor tissue for each group. Scale bar: 50 μm. (B–D) Statistical analyses of the percentage of positive staining area for Ki67, CD4, and CD8, respectively. Significant differences: $**P < 0.01$ and $***P < 0.001$.

cells, along with a reduction in tumor volume compared to the antibiotic-only groups. The contrasting trends in CD4+/CD8+ infiltration observed between Figs. 6 and 7 highlight the distinct immune contexts of the two independent mouse cohorts: antibiotic-induced immune suppression in the ATB group versus immune restoration in the DCA group, rather than reflecting inconsistent experimental outcomes. Although Ki67 levels in the DCA + PTX + αPD-1 group were not significantly lower than those in the DCA or control groups, this observation likely reflects the limited sensitivity of Ki67 as a static proliferation marker in regressed and partially necrotic tumors, rather than indicating a lack of therapeutic synergy. DCA supplementation in this study was performed in antibiotic-free mice and therefore does not directly test the reversal of ATB-induced immune suppression. Our findings should be interpreted as functional associations rather than definitive causation. Future work will evaluate DCA rescue after ATB exposure and investigate bile-acid signaling to establish causal mechanisms.

Studies have shown that antibiotics may alter the composition of the gut microbiota and affect the metabolic products of the microbiota, particularly short-chain fatty acids [21]. Short-chain fatty acids, including acetic acid and butyric acid, are among the main metabolic products of the gut microbiota and play important roles in promoting intestinal epithelial function and nutrient absorption and maintaining the integrity of the gut. These changes not only affect gut health but also may have an impact on systemic metabolism. In metabolomic studies, we identified DCA as a differentially abundant metabolite and found that it decreased significantly after the use of antibiotics, with this difference persisting until the end of chemoimmunotherapy. This result was confirmed in both mouse blood and human fecal samples. Our results suggest that antibiotics may regulate the efficacy of chemoimmunotherapy by affecting the levels of DCA. DCA, a secondary bile acid, has recently gained attention in the field of oncology because of its potential role in modulating the efficacy of cancer treatments, particularly in combination with immunotherapy [22]. A previous study reported that UDCA can inhibit proliferation and induce apoptosis in NSCLC cells and also reduce doxorubicin-induced autophagy by regulating the transforming growth factor-β/mitogen-activated protein kinase (TGF-β/MAPK) signaling axis and enhancing the efficacy of doxorubicin in NSCLC [23]. One of the mechanisms by which DCA influences treatment outcomes is through its effects on immune cell function [24, 25]. It has been reported that DCA can modulate the activity of various immune cells, including T cells and dendritic cells. By influencing the signaling pathways within these cells, DCA can enhance their ability to recognize and attack cancer cells. For example, DCA can stimulate the maturation of dendritic cells, which are essential for presenting tu-

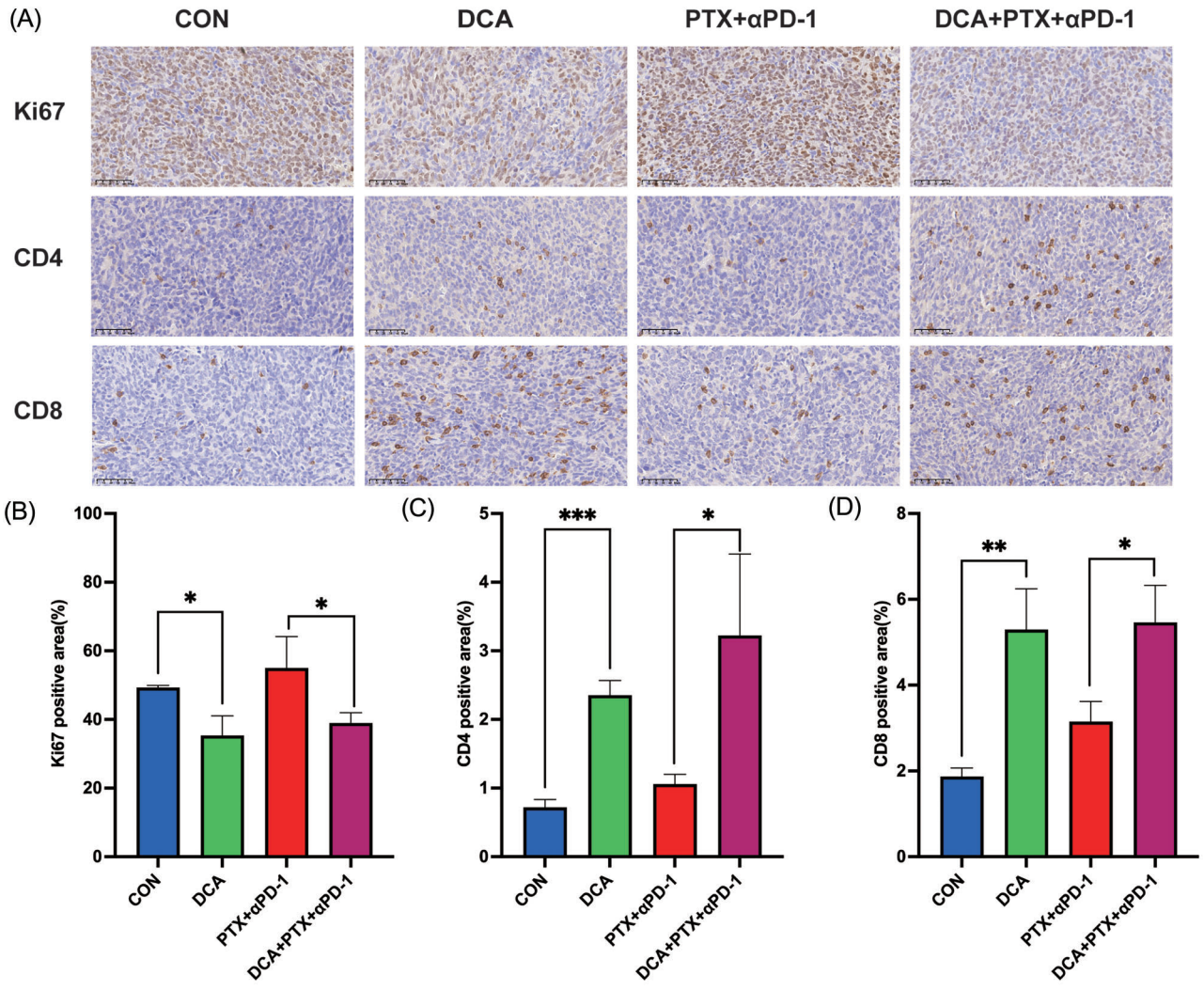

Figure 7 Influence of DCA pretreatment on the expression levels of Ki67, CD4, and CD8. (A) Immunohistochemical staining images of Ki67, CD4, and CD8 in subcutaneous tumor tissue (scale bar = 100 μm); (B–D) Statistics of positive regions of immunohistochemical proteins; $*P < 0.05$, $**P < 0.01$, $***P < 0.001$.

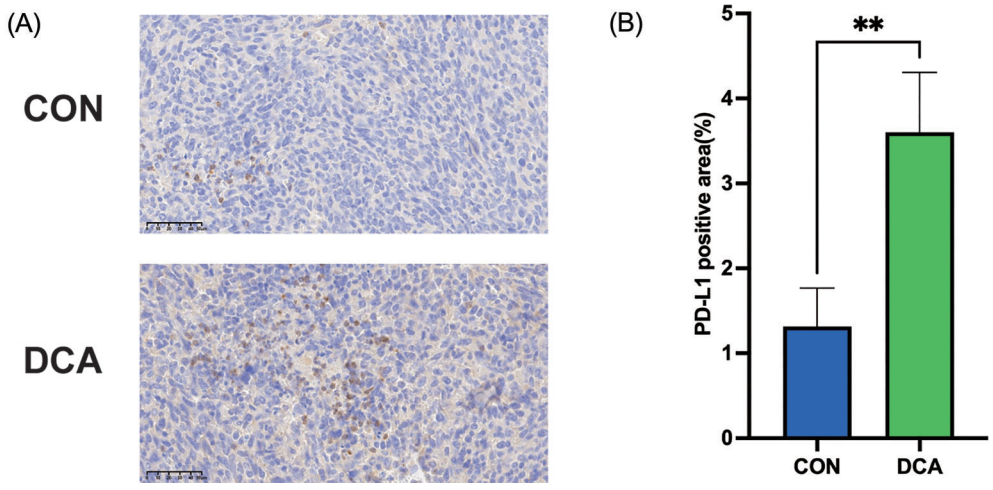

Figure 8 Effect of DCA treatment on the expression level of PD-L1. (A) Immunohistochemical staining images of PD-L1 in subcutaneous tumor tissue (scale bar = 100 μm); (B) statistics of positive regions of immunohistochemical proteins; $**P < 0.01$.

mor antigens to T cells, thereby initiating an adaptive immune response. Another significant way that DCA contributes to the efficacy of chemoimmunotherapy is by promoting the presentation of tumor antigens [24, 25]. Tumor cells often employ strategies to evade immune detection, but DCA can counteract these mechanisms. DCA can facilitate the release of tumor-associated antigens and increase their uptake by antigen-presenting cells. This process is critical for activating T-cell responses, which constitute the backbone of many immunotherapeutic strategies. The ability of DCA to modulate immune cell function and promote tumor antigen presentation suggests that DCA could be a valuable adjunct to chemoimmunotherapy.

Our research found that DCA promoted the increased expression of PD-L1. Clinical studies have shown that patients with high expression of PD-L1 (such as TPS $\geq$ 50%) have a higher response rate to ICIs (such as pembrolizumab) and a longer survival period. For instance, the Keynote 024 trial demonstrated that in NSCLC patients with high PD-L1 expression, pembrolizumab significantly prolonged PFS and OS compared with chemotherapy [26]. Chemotherapy drugs (such as paclitaxel, gemcitabine) or radiotherapy can induce PD-L1 expression through DNA damage or inflammatory signals (such as interferon-γ), enhancing the sensitivity to subsequent immunotherapy. For example, in the PACIFIC trial, the use of duvalizumab after radiotherapy and chemotherapy significantly prolonged survival [27]. Oncolytic viruses (such as talimogene laherparepvec) or local radiotherapy induce the expression of PD-L1 and enhance the abscopal effect [28]. However, there are exceptions. Some patients with high expression of PD-L1 may not respond to treatment, which may be related to other factors in the tumor microenvironment, such as insufficient T-cell infiltration and the existence of other immunosuppressive mechanisms. Therefore, although PD-L1 is an important biomarker, it is not the only determining factor. Actively promoting PD-L1 expression without combining it with immunotherapy may accelerate immunosuppression and promote tumor growth. Therefore, the key is that while promoting the expression of PD-L1, ICIs must be used in combination so that blocking the PD-L1/PD-1 pathway can translate into therapeutic effects.

Although our study provides new insights into the impact of antibiotic use on the efficacy of chemoimmunotherapy, several limitations should be acknowledged. First, antibiotic exposure was defined using a 30-day pre-treatment window, which may not fully capture the heterogeneity in antibiotic half-lives, the duration of microbiota disturbance, or recovery dynamics. Shorter or longer exposure windows may exert differential effects on gut microbial resilience and immune reconstitution, warranting further investigation in prospective studies. Second, although patients in the clinical cohort received diverse classes of antibiotics, the animal model employed a single broad-spectrum agent (ceftriaxone) to induce gut microbiota dysbiosis. This approach was intended to model antibiotic-induced microbial disruption in a controlled manner rather than to replicate the full clinical heterogeneity of antibiotic regimens. Future studies incorporating multiple antibiotics and varying exposure durations will be necessary to validate the generalizability of these findings. In addition, although differential gut microbiota composition and bile acid-related metabolites were identified in the mouse models, the number of human samples was limited, which may restrict the broader applicability of our results. Larger, well-characterized clinical cohorts are therefore needed to confirm these observations and to better delineate inter-individual variability. Finally, mechanistic validation in the present study was limited. While immunohistochemical analyses of CD4+/CD8+ T-cell infiltration and Ki67 expression provided important insights into the immune contexture and tumor proliferative status, functional characterization of immune cells was not performed. Moreover, although 16S rRNA sequencing revealed antibiotic-associated shifts in microbial community structure, functional gene alterations and metabolic pathway changes were not directly assessed, and potential direct effects of antibiotics on intestinal epithelial integrity could not be excluded. Accordingly, our findings should be interpreted as supporting a functional association, rather than a fully delineated molecular mechanism, linking antibiotic exposure to impaired antitumor immunity.

Future work incorporating flow cytometry, multiplex immunofluorescence, metagenomic sequencing, and metabolomic analyses will be required to characterize immune functional states and microbial metabolic capacity, and to distinguish immune-mediated modulation from potential direct tissue effects. These studies will further elucidate how antibiotics modulate the tumor immune microenvironment and influence the efficacy of chemoimmunotherapy, potentially informing novel therapeutic strategies.

Conclusions

Our study emphasized the importance of considering antibiotic use in combination with chemoimmunotherapy and revealed the potential mechanisms by which antibiotics may regulate treatment outcomes by affecting the gut microbiota and its metabolite DCA. These findings provide new directions for future research and may have a significant impact on clinical treatment practices.

Acknowledgements

This study was supported by the National Natural Science Foundation of China (grant No. 82370085 to C.C.), Wujieping Medical Foundation Clinical Research Special Fund (grant No. 320.6750.2025–6-88 to Y.L.), and Wenzhou Municipal Science and Technology Bureau (grant No. Y2020001 to H.X.). We are grateful for all the financial support of this study and to the participants in the study.

Author contributions

Hanyan Xu (Conceptualization, Formal Analysis, Methodology, Writing—original draft, Writing—review & editing), Jia Yu (Conceptualization, Formal Analysis, Methodology, Writing—original draft, Writing—review & editing), Lijing Xia (Formal Analysis, Validation), Xiong Lei (Formal Analysis, Investigation), Liwen Zhou (Methodology, Visualization), Pengcheng Lin (Formal Analysis, Methodology), Shanshan Su (Formal Analysis, Supervision), Yuping Li (Conceptualization, Writing—review & editing), and Chengshui Chen (Conceptualization, Writing—review & editing).

Supplementary material

Supplementary material is available at *PCMEDI* online.

Conflicts of interest

None declared.

Ethics statement

This study was approved by the ethics committee of the First Affiliated Hospital of Wenzhou Medical University (ethics approval No. 2020084) and complies with the declaration of Helsinki. Informed consent was obtained from all participants.

References

1. Kim H, Lee JE, Hong SH *et al.* The effect of antibiotics on the clinical outcomes of patients with solid cancers undergoing immune checkpoint inhibitor treatment: a retrospective study. *BMC Cancer* 2019;**19**:1100. https://doi.org/10.1186/s12885-019-6267-z
2. Hakozaki T, Okuma Y, Omori M *et al.* Impact of prior antibiotic use on the efficacy of nivolumab for non-small cell lung cancer. *Oncol Lett* 2019;**17**:2946–52. https://doi.org/10.3892/ol.2019.9899
3. Lurienne L, Cervesi J, Duhalde L *et al.* NSCLC Immunotherapy efficacy and antibiotic use: A systematic review and meta-analysis. *J Thorac Oncol* 2020;**15**:1147–59. https://doi.org/10.1016/j.jtho.2020.03.002
4. Tinsley N, Zhou C, Tan G *et al.* Cumulative antibiotic use significantly decreases efficacy of checkpoint inhibitors in patients with advanced cancer. *Oncologist* 2020;**25**:55–63. https://doi.org/10.1634/theoncologist.2019-0160
5. Pinato DJ, Howlett S, Ottaviani D *et al.* Association of prior antibiotic treatment with survival and response to Immune checkpoint inhibitor therapy in patients with cancer. *JAMA Oncol* 2019;**5**:1774–8. https://doi.org/10.1001/jamaoncol.2019.2785
6. Xin Y, Liu CG, Zang D *et al.* Gut microbiota and dietary intervention: affecting immunotherapy efficacy in non-small cell lung cancer. *Front Immunol* 2024;**15**:1343450. https://doi.org/10.3389/fimmu.2024.1343450
7. Almonte AA, Rangarajan H, Yip D *et al.* How does the gut microbiome influence immune checkpoint blockade therapy? *Immunol Cell Biol* 2021;**99**:361–72. https://doi.org/10.1111/imcb.12423
8. Routy B, Le Chatelier E, Derosa L *et al.* Gut microbiome influences efficacy of PD-1-based immunotherapy against epithelial tumors. *Science* 2018;**359**:91–7. https://doi.org/10.1126/science.aan3706
9. Ju L, Suo Z, Lin J *et al.* Fecal microbiota and metabolites in the pathogenesis and precision medicine for inflammatory bowel disease. *Precis Clin Med* 2024;**7**:pbae023. https://doi.org/10.1093/pcmedi/pbae023
10. Liu F, Li J, Guan Y *et al.* Dysbiosis of the gut microbiome is associated with tumor biomarkers in lung cancer. *Int J Biol Sci* 2019;**15**:2381–92. https://doi.org/10.7150/ijbs.35980
11. Jia D, Wang Q, Qi Y *et al.* Microbial metabolite enhances immunotherapy efficacy by modulating T cell stemness in pan-cancer. *Cell* 2024;**187**:1651–65. https://doi.org/10.1016/j.cell.2024.02.022
12. West H, McCleod M, Hussein M *et al.* Atezolizumab in combination with carboplatin plus nab-paclitaxel chemotherapy compared with chemotherapy alone as first-line treatment for metastatic non-squamous non-small-cell lung cancer (IMpower130): a multicentre, randomised, open-label, phase 3 trial. *Lancet Oncol* 2019;**20**:924–37. https://doi.org/10.1016/S1470-2045(19)30167-6
13. Paz-Ares L, Vicente D, Tafreshi A *et al.* A randomized, placebo-controlled trial of Pembrolizumab Plus Chemotherapy in patients with metastatic squamous NSCLC: protocol-specified final analysis of KEYNOTE-407. *J Thorac Oncol* 2020;**15**:1657–69. https://doi.org/10.1016/j.jtho.2020.06.015
14. Xiong F, Gong K, Xu H *et al.* Optimized integration of metabolomics and lipidomics reveals brain region-specific changes of oxidative stress and neuroinflammation in type 1 diabetic mice with cognitive decline. *J Adv Res* 2023;**43**:233–45. https://doi.org/10.1016/j.jare.2022.02.011
15. Cortellini A, Ricciuti B, Facchinetti F *et al.* Antibiotic-exposed patients with non-small-cell lung cancer preserve efficacy outcomes following first-line chemo-immunotherapy. *Ann Oncol* 2021;**32**:1391–9. https://doi.org/10.1016/j.annonc.2021.08.1744
16. Gandhi L, Rodriguez-Abreu D, Gadgeel S *et al.* Pembrolizumab plus chemotherapy in metastatic non-small-cell lung cancer. *N Engl J Med* 2018;**378**:2078–92. https://doi.org/10.1056/NEJMoa1801005
17. Cortellini A, Facchinetti F, Derosa L *et al.* Antibiotic exposure and immune checkpoint inhibitors in patients with NSCLC: the backbone matters. *J Thorac Oncol* 2022;**17**:739–41. https://doi.org/10.1016/j.jtho.2022.03.016
18. Cortellini A, Di Maio M, Nigro O *et al.* Differential influence of antibiotic therapy and other medications on oncological outcomes of patients with non-small cell lung cancer treated with first-line pembrolizumab versus cytotoxic chemotherapy. *J Immunother Cancer* 2021;**9**:e002421. https://doi.org/10.1136/jitc-2021-002421
19. Willmann M, Vehreschild M, Biehl LM *et al.* Distinct impact of antibiotics on the gut microbiome and resistome: a longitudinal multicenter cohort study. *BMC Biol* 2019;**17**:76. https://doi.org/10.1186/s12915-019-0692-y
20. Ramirez J, Guarner F, Bustos Fernandez L *et al.* Antibiotics as major disruptors of gut microbiota. *Front Cell Infect Microbiol* 2020;**10**:572912. https://doi.org/10.3389/fcimb.2020.572912
21. Pauline M, Fouhse J, Hinchliffe T *et al.* Probiotic treatment vs empiric oral antibiotics for managing dysbiosis in short bowel syndrome: impact on the mucosal and stool microbiota, short-chain fatty acids, and adaptation. *JPEN J Parenter Enteral Nutr* 2022;**46**:1828–38. https://doi.org/10.1002/jpen.2377
22. Lu Y, Feng X, Wang Z *et al.* Bile acid metabolism and hepatocellular carcinoma: mechanisms of drug resistance and intervention strategies. *Precis Clin Med* 2025;**8**:pbaf020. https://doi.org/10.1093/pcmedi/pbaf020
23. Li Y, Zhao H, Shen Z *et al.* Enhancing DOX efficacy against NSCLC through UDCA-mediated modulation of the TGF-beta/MAPK autophagy pathways. *Sci Rep* 2024;**14**:27169. https://doi.org/10.1038/s41598-024-73736-7
24. Kiriyama Y, Nochi H. The role of gut microbiota-derived lithocholic acid, deoxycholic acid and their derivatives on the function and differentiation of immune cells. *Microorganisms* 2023;**11**:2730. https://doi.org/10.3390/microorganisms11112730

25. Kim J, Kang S, Kim J *et al.* Dual adjuvant-loaded peptide antigen self-assembly potentiates dendritic cell-mediated tumor immunotherapy. *Adv Sci (Weinh)* 2024;**11**:e2403663. https://doi.org/10.1002/advs.202403663
26. Reck M, Rodriguez-Abreu D, Robinson AG *et al.* Updated analysis of KEYNOTE-024: Pembrolizumab versus platinum-based chemotherapy for advanced non-small-cell lung cancer with PD-L1 tumor proportion score of 50% or greater. *J Clin Oncol* 2019;**37**:537–46. https://doi.org/10.1200/JCO.18.00149
27. Spigel DR, Faivre-Finn C, Gray JE *et al.* Five-year survival outcomes from the PACIFIC trial: Durvalumab after chemoradiotherapy in stage III non-small-cell lung cancer. *J Clin Oncol* 2022;**40**:1301–11. https://doi.org/10.1200/jco.21.01308
28. Ribas A, Dummer R, Puzanov I *et al.* Oncolytic virotherapy promotes intratumoral T cell infiltration and improves Anti-PD-1 immunotherapy. *Cell* 2017;**170**:1109–19. https://doi.org/10.1016/j.cell.2017.08.027

Received: 19 August 2025. **Revised:** 23 December 2025. **Accepted:** 3 January 2026